

Investigation into Diphosphine Oxides as Ligands in Diorganotin(IV) Adducts. Part 2.¹ Synthesis, Spectroscopic Characterization, and X-Ray Crystal Structure of *cis*-1,2-Bis(diphenylphosphoryl)ethylenetin Complexes †

Philip G. Harrison and Nelson W. Sharpe

Department of Chemistry, University of Nottingham, University Park, Nottingham NG7 2RD

Corrado Pelizzi, Giancarlo Pelizzi,* and Pieralberto Tarasconi

Istituto di Chimica Generale ed Inorganica, Centro di Studio per la Strutturistica Diffraattometrica del CNR, Via M. D'Azeglio 85, 43100 Parma, Italy

Organotin(IV) complexes of formula $\text{SnR}_2\text{Cl}_2(\text{dp}(\text{poet}))$ [$\text{dp}(\text{poet}) = \text{cis-1,2-bis(diphenylphosphoryl)ethylene}$; $\text{R} = \text{Bu}^n, \text{Pr}^n, \text{or Ph}$] have been synthesised and characterised by i.r. and tin-119 Mössbauer spectroscopies. An X-ray diffraction analysis has been carried out on $\text{SnBu}^n_2\text{Cl}_2(\text{dp}(\text{poet}))$ (1) and $\text{SnPr}^n_2\text{Cl}_2(\text{dp}(\text{poet}))$ (2). Both compounds crystallize in the monoclinic system with $a = 13.76(1)$, $b = 15.29(1)$, $c = 18.36(1)$ Å, $\beta = 113.70(9)^\circ$, $Z = 4$, and space group $P2_1/c$ for (1) and $a = 11.362(4)$, $b = 16.816(4)$, $c = 9.324(3)$ Å, $\beta = 108.94(3)^\circ$, $Z = 2$, and space group $P2_1$ for (2). The structures have been determined using diffractometer data and refined to conventional R factors of 0.0979 for (1) and 0.0532 for (2) (3 113 and 2 233 reflections, respectively). The major difference between the two structures is associated with behaviour of the $\text{dp}(\text{poet})$ ligand, *i.e.* symmetrically bidentate in (1) and predominantly unidentate in (2). Tin-119 Mössbauer spectra have been recorded for both (1) and (2) in the temperature range 77–150 K. Quadrupole splitting values of *ca.* 4 mm s^{-1} are in accord with the *trans*- SnR_2X_4 geometry deduced from the X-ray studies, whilst the values of the temperature coefficients of the recoil-free fraction are characteristic of molecular lattices, the lower value for (2) being attributed to the more open co-ordination of the tin atom in this complex.

Diphosphine oxides show interesting co-ordinating behaviour in metal complexes as can be observed from the few structural studies reported in the literature.²⁻⁷

The investigation we have carried out on organotin(IV) derivatives with $\text{OP}(\text{Ph})_2\text{-R-(Ph)}_2\text{PO}$ diphosphine oxides has revealed that the chelating properties of the P ligands are influenced by the nature of the R group as well as by the nature of the organotin compound. An unusual unidentate behaviour has been observed by us for *cis*-1,2-bis(diphenylphosphoryl)ethylene ($\text{dp}(\text{poet})$) in $\text{SnPh}_3\text{Cl}(\text{dp}(\text{poet}))$.⁸

Recently we have reported the synthesis, the characterization by i.r. spectra and ¹¹⁹Sn Mössbauer spectroscopies, and the X-ray diffraction analysis of a series of organotin(IV) adducts with 1,2-bis(diphenylphosphoryl)ethane ($\text{dp}(\text{poe})$).^{1,7}

The present work deals with the syntheses and the characterization by i.r. and ¹¹⁹Sn Mössbauer techniques of three new adducts of formula $\text{SnR}_2\text{Cl}_2(\text{dp}(\text{poet}))$ [$\text{R} = \text{Bu}^n$ (1), Pr^n (2), or Ph] and of the complex $\text{SnPh}_3\text{Cl}(\text{dp}(\text{poet}))$. The X-ray diffraction analyses of the *n*-butyl- and the *n*-propyl-tin derivatives are also presented.

Experimental

Preparations.—Toluene and acetone were dried over sodium and 4 Å molecular sieves respectively, and distilled prior to use. *cis*-1,2-Bis(diphenylphosphino)ethylene and organotin chlorides were purchased from Strem Chemical Co. and used without further purification. *cis*-1,2-Bis(diphenylphosphoryl)ethylene ($\text{dp}(\text{poet})$) was obtained by refluxing for 1 h a toluene solution of *cis*-1,2-bis(diphenylphosphino)ethylene with H_2O_2 (31.5%) in excess.⁹ The complex $\text{SnPh}_3\text{Cl}(\text{dp}(\text{poet}))$

Table 1. Analytical data (%)^a

	C	H	Sn ^b
$\text{SnPh}_2\text{Cl}_2(\text{dp}(\text{poet}))$	59.15 (59.10)	4.20 (4.20)	<i>ca.</i> 15 (15.40)
$\text{SnPr}^n_2\text{Cl}_2(\text{dp}(\text{poet}))$	55.05 (54.60)	5.45 (5.15)	<i>ca.</i> 15 (16.90)
$\text{SnPh}_3\text{Cl}(\text{dp}(\text{poet}))$	65.20 (64.95)	4.65 (4.60)	— —

^a Calculated values in parentheses. ^b By atomic absorption spectroscopy.

was prepared as described elsewhere.⁸ Diorganotin(IV) adducts were prepared by adding an acetone solution of SnR_2Cl_2 to a toluene solution of $\text{dp}(\text{poet})$ in 1:1 mol ratio. The solution was stirred at room temperature for 1 h and then allowed to stand. Solvents were slowly evaporated in air until a white crystalline product was isolated.

Measurements.—Elemental C and H analyses were made on Perkin-Elmer model 240 automatic equipment and are given in Table 1. Infrared spectra (4 000–200 cm^{-1}) were recorded on a Perkin-Elmer model 283 B instrument using KBr discs.

The procedures employed for the collection of ¹¹⁹Sn Mössbauer spectra have been reported previously.¹ Spectra for the two complexes $\text{SnPr}^n_2\text{Cl}_2(\text{dp}(\text{poet}))$ and $\text{SnBu}^n_2\text{Cl}_2(\text{dp}(\text{poet}))$ were recorded at various temperatures in the range 77–150 K, accumulating a minimum of 10⁶ counts per channel, and subsequently fitted to Lorentzian lineshapes by usual least-squares methods.

X-Ray Data Collection, and Determination and Refinement of the Crystal Structures of $\text{SnBu}^n_2\text{Cl}_2(\text{dp}(\text{poet}))$ (1) and $\text{SnPr}^n_2\text{Cl}_2(\text{dp}(\text{poet}))$ (2).—Both compounds crystallize in the monoclinic system: the systematic absences ($h0l$, $l \neq 2n$, and $0k0$, $k \neq 2n$) uniquely conform to the space group $P2_1/c$ in (1), while for (2) the extinctions $0k0$, $k \neq 2n$, allow the space

† [*cis*-1,2-Bis(diphenylphosphoryl)ethylene-*OO'*]di-*n*-butyldichlorotin(IV) and [*cis*-1,2-bis(diphenylphosphoryl)ethylene-*O*]dichloro-*n*-propyltin(IV).

Supplementary data available (No. SUP 23605, 36 pp.): observed and calculated structure factors, thermal parameters. See Notices to Authors No. 7, *J. Chem. Soc., Dalton Trans.*, 1981, Index issue.

group to be $P2_1$ or $P2_1/m$, the former being assumed in the initial stages on the basis of the E statistics and shown to be correct by the successful refinement. Data were collected at room temperature with a computer-controlled Siemens AED single-crystal diffractometer using nickel-filtered Cu-K_α radiation. The intensity of each reflection was obtained from a profile analysis following the Lehmann and Larsen notation¹⁰ with a program written by Belletti *et al.*¹¹ A summary of the most significant crystallographic data and the experimental conditions for intensity data collection are given in Table 2 for the two compounds.

The intensity of a standard reflection, monitored at intervals of every 50 reflections, decreased with time dramatically for (1) and at a smaller extent for (2). These effects, which were undoubtedly a sign of the decomposition of the specimens in the X-ray beam, were allowed for by scaling the reflections with respect to the standards. Corrections were made for Lorentz and polarization effects, but not for absorption, as decomposition effects prevented a precise measurement of the

faces, and the size of the crystals satisfied the condition $\mu\bar{r} \approx 0.5$ (\bar{r} = radius in cm).

The solution of the structure of compound (1) was achieved using a combination of direct methods and the Fourier techniques. The Sn, Cl, and P atom positions were located by multi-solution Σ_2 sign expansion, and all the remaining non-hydrogen atoms were found through subsequent difference-Fourier syntheses. The structure was refined by full-matrix least squares, treating the phenyl rings as rigid bodies and with all atoms other than the C atoms of the butyl groups given anisotropic thermal parameters. Out of the 40 hydrogen atoms, only the two ethylene H atoms were located in a ΔF map and their parameters were allowed to refine isotropically. The somewhat large R value of 0.0979 is due to some extent to decomposition effects. Nine reflections, with high discrepancies between F_o and F_c , were omitted from the last calculations. The strongest feature on the final ΔF map was two peaks of height $1.1 \text{ e } \text{\AA}^{-3}$ in the vicinity of tin, all other residual peaks were smaller than $0.4 \text{ e } \text{\AA}^{-3}$.

The structure of compound (2) was solved by the heavy-atom technique. The tin atom was located by means of a Patterson function and the remaining non-hydrogen atoms from subsequent electron-density difference syntheses. Three cycles of full-matrix least-squares refinement with all the non-hydrogen atoms assigned anisotropic thermal parameters, with the atoms of the four phenyl rings refined freely and with the H atoms from the ethylene moiety as isotropic atoms, led to convergence with $R = 0.0532$. The final-difference map showed two peaks of $1.6 \text{ e } \text{\AA}^{-3}$ within 1.0 \AA of tin, the residual peaks were all less than $0.4 \text{ e } \text{\AA}^{-3}$.

In both compounds the quantity minimized was $\Sigma w(F_o - F_c)^2$, in which the weighting scheme $w = [\sigma^2(F_o) + 0.005|F_o|^2]^{-1}$ was employed in the final stages of refinement. Neutral-atom scattering factors were used throughout, those for the non-hydrogen atoms being corrected for anomalous dispersion. All computations were completed using the SHELX 76 program set¹² on the Cyber 76 Computer of CINECA (Casalecchio, Bologna), with financial support from the University of Parma.

Fractional atomic co-ordinates for the two structures are given in Tables 3 and 4. Tables 5 and 6 contain selected bond distances and angles for (1) and (2), respectively.

Table 2. Crystallographic data

Compound	$\text{SnBu}^n_2\text{Cl}_2(\text{dp}^n\text{poet})$	$\text{SnPr}^n_2\text{Cl}_2(\text{dp}^n\text{poet})$
Formula	$\text{C}_{34}\text{H}_{40}\text{Cl}_2\text{O}_2\text{P}_2\text{Sn}$	$\text{C}_{32}\text{H}_{36}\text{Cl}_2\text{O}_2\text{P}_2\text{Sn}$
M	732.23	704.18
Crystal system	Monoclinic	Monoclinic
Space group	$P2_1/c$	$P2_1$
$a/\text{\AA}$	13.76(1)	11.362(4)
$b/\text{\AA}$	15.29(1)	16.816(4)
$c/\text{\AA}$	18.36(1)	9.324(3)
$\beta/^\circ$	113.70(9)	108.94(3)
$U/\text{\AA}^3$	3 537(6)	1 685(1)
Z	4	2
$D_c/\text{g cm}^{-3}$	1.375	1.388
$F(000)$	1 496	716
X-radiation, $\lambda/\text{\AA}$	Cu-K_α , 1.541 78	Cu-K_α , 1.541 78
Dimensions/mm	$0.09 \times 0.16 \times 0.65$	$0.08 \times 0.13 \times 0.34$
μ/cm^{-1}	83.9	87.9
2θ limit/ $^\circ$	0–112	6–132
Total data measured	5 677	3 226
Total unique data	5 262	3 022
Data with $I > 2\sigma(I)$	3 113	2 233
R	0.0979	0.0532

Table 3. Fractional atomic co-ordinates ($\times 10^4$) with e.s.d.s in parentheses for $\text{SnBu}^n_2\text{Cl}_2(\text{dp}^n\text{poet})$

Atom	X/a	Y/b	Z/c	Atom	X/a	Y/b	Z/c
Sn	2 622(1)	2 595(1)	1 621(1)	C(24)	4 394(7)	6 159(5)	155(7)
Cl(1)	2 991(3)	1 290(3)	2 540(3)	C(25)	4 244(7)	5 789(5)	797(7)
Cl(2)	3 213(3)	3 789(3)	2 644(3)	C(26)	3 569(7)	5 073(5)	677(7)
P(1)	2 104(3)	1 365(2)	–204(3)	C(27)	918(6)	4 067(6)	–919(7)
P(2)	2 191(3)	3 790(2)	–199(2)	C(28)	109(6)	4 232(6)	–663(7)
O(1)	2 053(6)	1 673(7)	546(7)	C(29)	–897(6)	4 471(6)	–1 211(7)
O(2)	2 148(8)	3 539(7)	579(6)	C(30)	–1 095(6)	4 545(6)	–2 016(7)
C(9)	2 918(7)	412(6)	–31(7)	C(31)	–286(6)	4 380(6)	–2 272(7)
C(10)	3 104(7)	7(6)	–644(7)	C(32)	721(6)	4 140(6)	–1 724(7)
C(11)	3 775(7)	–717(6)	–481(7)	C(33)	2 628(9)	2 135(9)	–681(8)
C(12)	4 260(7)	–1 035(6)	294(7)	C(34)	2 675(10)	3 009(8)	–690(8)
C(13)	4 075(7)	–630(6)	907(7)	C(1)	4 134(14)	2 550(10)	1 546(12)
C(14)	3 403(7)	94(6)	744(7)	C(2)	5 025(21)	2 427(14)	2 321(17)
C(15)	800(5)	1 098(6)	–928(6)	C(3)	6 048(27)	2 609(17)	2 201(21)
C(16)	308(5)	355(6)	–792(6)	C(4)	6 785(27)	2 056(22)	2 781(22)
C(17)	–748(5)	176(6)	–1 281(6)	C(5)	1 044(17)	2 800(13)	1 515(14)
C(18)	–1 311(5)	739(6)	–1 906(6)	C(6)	167(22)	2 353(15)	849(18)
C(19)	–819(5)	1 482(6)	–2 042(6)	C(7)	–941(25)	2 555(15)	883(21)
C(20)	236(5)	1 661(6)	–1 553(6)	C(8)	–1 671(25)	2 280(19)	121(20)
C(21)	3 045(7)	4 727(5)	–84(7)	H(33)	2 973(113)	1 796(103)	–1 049(103)
C(22)	3 195(7)	5 096(5)	–725(7)	H(34)	2 884(116)	3 087(108)	–1 242(106)
C(23)	3 870(7)	5 812(5)	–606(7)				

Table 4. Fractional atomic co-ordinates ($\times 10^4$) with e.s.d.s in parentheses for $\text{SnPr}^n_2\text{Cl}_2(\text{dppoet})$

Atom	X/a	Y/b	Z/c	Atom	X/a	Y/b	Z/c
Sn	1 718(1)	2 500(0)	1 430(1)	C(15)	-334(21)	-614(12)	2 715(26)
Cl(1)	-107(3)	2 629(3)	-823(4)	C(16)	638(18)	-964(9)	3 925(25)
Cl(2)	3 222(3)	3 089(2)	175(4)	C(17)	1 326(17)	-527(9)	5 159(22)
P(1)	48(3)	1 721(2)	3 865(3)	C(18)	1 134(13)	300(7)	5 199(17)
P(2)	3 350(3)	2 261(2)	5 768(4)	C(19)	4 112(15)	3 193(10)	6 356(16)
O(1)	402(8)	2 075(6)	2 606(9)	C(20)	5 368(19)	3 242(17)	6 534(26)
O(2)	3 109(8)	2 099(6)	4 115(10)	C(21)	5 990(27)	3 990(23)	6 969(34)
C(1)	1 800(17)	3 618(7)	2 563(17)	C(22)	5 239(38)	4 649(19)	7 072(28)
C(2)	1 386(18)	4 348(7)	1 590(22)	C(23)	3 967(27)	4 615(13)	6 911(24)
C(3)	1 493(19)	5 070(11)	2 624(25)	C(24)	3 426(20)	3 866(10)	6 578(21)
C(4)	2 291(14)	1 318(8)	1 094(16)	C(25)	4 242(14)	1 503(10)	6 945(18)
C(5)	1 749(20)	946(10)	-341(19)	C(26)	4 325(17)	748(12)	6 247(23)
C(6)	2 107(20)	87(11)	-447(22)	C(27)	5 002(27)	133(14)	7 234(40)
C(7)	-1 546(11)	1 940(8)	3 582(14)	C(28)	5 518(24)	225(16)	8 741(32)
C(8)	-2 147(14)	1 650(9)	4 529(18)	C(29)	5 469(24)	976(14)	9 378(27)
C(9)	-3 387(14)	1 826(11)	4 327(24)	C(30)	4 856(19)	1 596(13)	8 541(21)
C(10)	-4 043(15)	2 347(9)	3 098(23)	C(31)	850(10)	2 098(7)	5 754(13)
C(11)	-3 429(15)	2 664(12)	2 217(21)	C(32)	2 020(11)	2 305(5)	6 443(12)
C(12)	-2 159(11)	2 480(14)	2 377(15)	H(31)	84(120)	2 090(90)	5 801(140)
C(13)	249(12)	663(7)	3 985(17)	H(32)	2 250(120)	2 511(80)	7 557(140)
C(14)	-521(16)	216(9)	2 783(19)				

Table 5. Selected bond distances (Å) and angles ($^\circ$) for $\text{SnBu}^n_2\text{Cl}_2(\text{dppoet})$

Sn-Cl(1)	2.529(5)	Sn-O(1)	2.29(1)	Sn-C(1)	2.14(2)
Sn-Cl(2)	2.509(5)	Sn-O(2)	2.27(1)	Sn-C(5)	2.12(2)
P(1)-O(1)	1.48(1)	P(1)-C(9)	1.79(1)	P(2)-C(21)	1.81(1)
P(2)-O(2)	1.50(1)	P(1)-C(15)	1.80(1)	P(2)-C(27)	1.77(1)
C(33)-C(34)	1.34(2)	P(1)-C(33)	1.78(1)	P(2)-C(34)	1.78(1)
Cl(1)-Sn-Cl(2)	99.0(2)	Cl(2)-Sn-O(1)	171.1(3)	O(1)-Sn-C(1)	85.9(6)
Cl(1)-Sn-O(1)	89.8(3)	Cl(2)-Sn-O(2)	93.7(3)	O(1)-Sn-C(5)	91.7(7)
Cl(1)-Sn-O(2)	167.2(3)	Cl(2)-Sn-C(1)	92.3(5)	O(2)-Sn-C(1)	85.6(6)
Cl(1)-Sn-C(1)	94.5(5)	Cl(2)-Sn-C(5)	88.4(6)	O(2)-Sn-C(5)	83.8(7)
Cl(1)-Sn-C(5)	95.8(6)	O(1)-Sn-O(2)	77.4(4)	C(1)-Sn-C(5)	169.4(8)
O(1)-P(1)-C(9)	110.7(6)	O(2)-P(2)-C(21)	111.3(6)	Sn-O(1)-P(1)	150.1(7)
O(1)-P(1)-C(15)	110.6(6)	O(2)-P(2)-C(27)	111.4(6)	Sn-O(2)-P(2)	148.7(7)
O(1)-P(1)-C(33)	115.2(7)	O(2)-P(2)-C(34)	118.4(6)	P(1)-C(33)-C(34)	134(1)
C(9)-P(1)-C(15)	108.3(5)	C(21)-P(2)-C(27)	107.4(5)	P(2)-C(34)-C(33)	129(1)
C(9)-P(1)-C(33)	106.1(6)	C(21)-P(2)-C(34)	103.4(6)	Sn-C(1)-C(2)	113(2)
C(15)-P(1)-C(33)	105.5(6)	C(27)-P(2)-C(34)	104.0(6)	Sn-C(5)-C(6)	117(2)

Results and Discussion

From the analytical data, the mol ratio of tin and diphosphine oxide was found to be the same (1 : 1) in all the complexes in spite of the amounts of the reagents used during the preparation.

The complexes can also be obtained from the reaction of the organotin compound with *cis*-1,2-bis(diphenylphosphino)ethylene by causing the oxidation of the P ligand after exposure in air for several days.

Infrared Spectra.—In this section we describe the i.r. spectrum of $\text{SnPh}_3\text{Cl}(\text{dppoet})$, whose synthesis and X-ray structure have been earlier reported,⁸ together with the spectra of the $\text{SnR}_2\text{Cl}_2(\text{dppoet})$ ($\text{R} = \text{Bu}^n, \text{Pr}^n, \text{or Ph}$) complexes. The almost complete analogy of the i.r. spectra of $\text{SnR}_2\text{Cl}_2(\text{dppoet})$ is noteworthy, the only small differences lie in the far-i.r. region. This spectral similarity can be justified by a similar stereochemistry involving the ligand behaviour of the diphosphine oxide. The position and the intensity of the $\nu(\text{P}=\text{O})$ stretching frequencies suggest the participation of the oxygen atom in the co-ordination to tin, in accord with values previously reported for similar complexes.¹³⁻¹⁵ There is no spectral evidence which can justify the differences in the

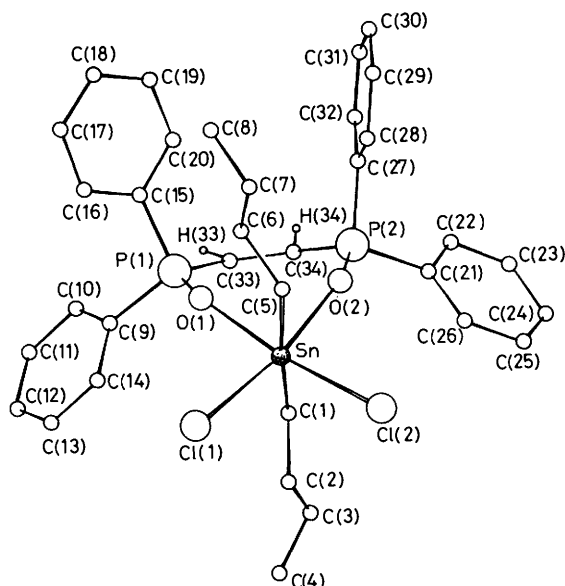
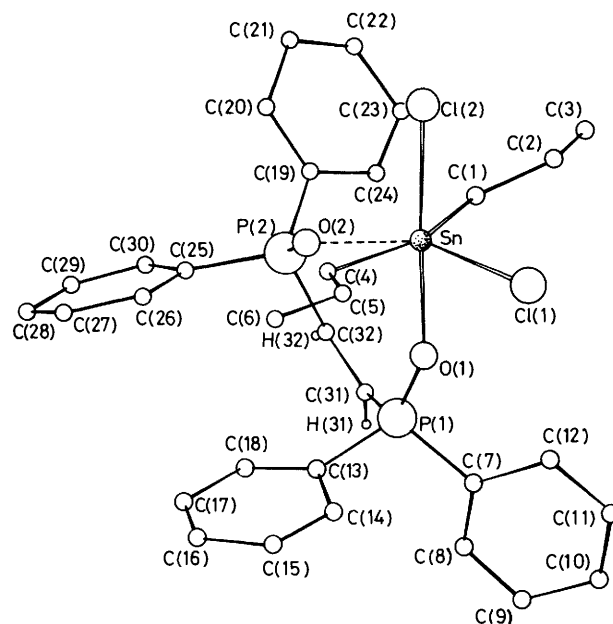
co-ordination polyhedron of the propyl and the butyl complexes as far as the Sn-O bond distances are concerned. The assignment of the medium band at *ca.* 595 cm^{-1} to the $\nu(\text{Sn}-\text{C})$ stretching mode in the two phenyl derivatives is consistent with that made for other analogous complexes.^{16,17} A contribution of the $\nu(\text{Sn}-\text{O})$ stretching mode to this broad band is also possible.¹⁸ Whilst no bands attributable to $\nu(\text{Sn}-\text{Cl})$ modes are present in the spectrum of (2), in that of (1) only a weak absorption at 340 cm^{-1} occurs, which can be assigned to the $\nu(\text{Sn}-\text{Cl})$ vibration.

The attributions of the vibrational bands involving the tin atom for the two phenyl derivatives are in agreement with those proposed for similar compounds.^{19,20} The spectrum of $\text{SnPh}_3\text{Cl}(\text{dppoet})$ as compared to those of the $\text{SnR}_2\text{Cl}_2(\text{dppoet})$ complexes shows a higher number of $\nu(\text{P}=\text{O})$ absorptions, due to the presence of unco-ordinated and co-ordinated $\text{P}=\text{O}$ groups. A comparison of the i.r. bands of the dppoet ligand in these compounds with those in other metal complexes is difficult owing to the limited available data.^{13,14}

X-Ray Structures.—It seemed reasonable to expect that the n-butyl- and n-propyl-tin derivatives, having the same stoichiometry, $\text{SnR}_2\text{Cl}_2(\text{dppoet})$, would have essentially

Table 6. Selected bond distances (Å) and angles (°) for $\text{SnPr}^n\text{Cl}_2(\text{dppoet})$

Sn-Cl(1)	2.436(3)	Sn-O(1)	2.24(1)	Sn-C(1)	2.14(1)
Sn-Cl(2)	2.563(4)	Sn-O(2)	2.58(1)	Sn-C(4)	2.15(1)
P(1)-O(1)	1.48(1)	P(1)-C(7)	1.78(1)	P(2)-C(19)	1.79(2)
P(2)-O(2)	1.50(1)	P(1)-C(13)	1.79(1)	P(2)-C(25)	1.77(1)
C(31)-C(32)	1.32(1)	P(1)-C(31)	1.81(1)	P(2)-C(32)	1.82(1)
Cl(1)-Sn-Cl(2)	94.5(1)	Cl(2)-Sn-O(1)	175.7(3)	O(1)-Sn-C(1)	88.1(5)
Cl(1)-Sn-O(1)	86.2(3)	Cl(2)-Sn-O(2)	104.8(5)	O(1)-Sn-C(4)	93.3(5)
Cl(1)-Sn-O(2)	160.5(4)	Cl(2)-Sn-C(1)	87.6(4)	O(2)-Sn-C(1)	80.6(6)
Cl(1)-Sn-C(1)	103.6(4)	Cl(2)-Sn-C(4)	90.7(4)	O(2)-Sn-C(4)	77.3(6)
Cl(1)-Sn-C(4)	99.8(4)	O(1)-Sn-O(2)	74.8(4)	C(1)-Sn-C(4)	156.6(6)
O(1)-P(1)-C(7)	108.9(6)	O(2)-P(2)-C(19)	112.5(7)	Sn-O(1)-P(1)	155.7(6)
O(1)-P(1)-C(13)	112.7(6)	O(2)-P(2)-C(25)	112.5(7)	Sn-O(2)-P(2)	143.1(6)
O(1)-P(1)-C(31)	116.6(6)	O(2)-P(2)-C(32)	117.9(6)	P(1)-C(31)-C(32)	132.3(9)
C(7)-P(1)-C(13)	108.5(6)	C(19)-P(2)-C(25)	108.6(7)	P(2)-C(32)-C(31)	129.7(9)
C(7)-P(1)-C(31)	103.7(6)	C(19)-P(2)-C(32)	103.4(6)	Sn-C(1)-C(2)	118(1)
C(13)-P(1)-C(31)	105.8(6)	C(25)-P(2)-C(32)	100.8(6)	Sn-C(4)-C(5)	119(1)

**Figure 1.** A perspective view of $\text{SnBu}^n\text{Cl}_2(\text{dppoet})$, showing the atom-numbering scheme**Figure 2.** A perspective view of $\text{SnPr}^n\text{Cl}_2(\text{dppoet})$, showing the atom-numbering scheme

similar structures. On the contrary, the *X*-ray analysis has revealed that the compounds show some significant differences which involve mainly the co-ordination mode of dppoet and, consequently, the geometry of the co-ordination polyhedron. In the butyl derivative (Figure 1), dppoet is symmetrically bidentately bonded to tin through its oxygen atoms at 2.27(1) and 2.29(1) Å, and, in this way, makes up an octahedral environment around tin comprising also two chlorine and two carbon atoms. The most distorted angles of the octahedron are O(1)-Sn-O(2) of 77.4(4)° and Cl(1)-Sn-O(2) of 167.2(3)°. The distortion from an ideal geometry probably arises as a consequence of a steric effect related to the different size of the donor atoms. In contrast, in (2) (Figure 2) the dppoet co-ordination is predominantly unidentate through O(1) [2.24(1) Å] with the other oxygen engaged in a rather long ligand to metal bond [Sn-O(2) 2.58(1) Å]. Thus the stereochemistry is basically five-co-ordinate, *i.e.* a distorted tetragonal pyramid with Cl(1) at the apex, but with O(2) occupying the sixth position to give a 4 + 1 + 1 co-ordination polyhedron. The two Sn-O bonds in (1) and the short Sn-O bond

in (2) are equal or somewhat longer than the 2.238(5) Å found in $[\text{SnPh}_3(\text{NO}_3)]_2(\text{dppoe})$,⁶ but are significantly shorter than the values observed in other dppoet or dppoet organotin(IV) adducts [*e.g.* 2.346(6) Å in $\text{SnPh}_3\text{Cl}(\text{dppoet})$,⁸ 2.357(3) Å in $(\text{SnPh}_3\text{Cl})_2(\text{dppoe})$,⁷ and 2.386(7) Å in $\text{SnBu}^n\text{Cl}_2(\text{dppoe})$].¹ As far as the long Sn-O bond in (2) is concerned, similar long values have been cited previously.¹ The Sn-Cl bonds show significant differences in the two structures. In (1) they are almost identical to within experimental error [2.509(5), 2.529(5) Å], while in (2) the unsymmetrical ligand co-ordination results in inequivalent Sn-Cl distances, 2.436(3) and 2.563(4) Å, with the shorter *trans* to the more loosely bonded oxygen atom. It can be added that the Sn-Cl bond distances in six-co-ordinate diorganotin adducts having two chlorines *cis* span the range 2.43–2.53 Å.¹

Within the two compounds the following common features involving the dppoet ligand may be noted: (*i*) the phosphorus atoms exhibit distorted tetrahedral geometries in which the

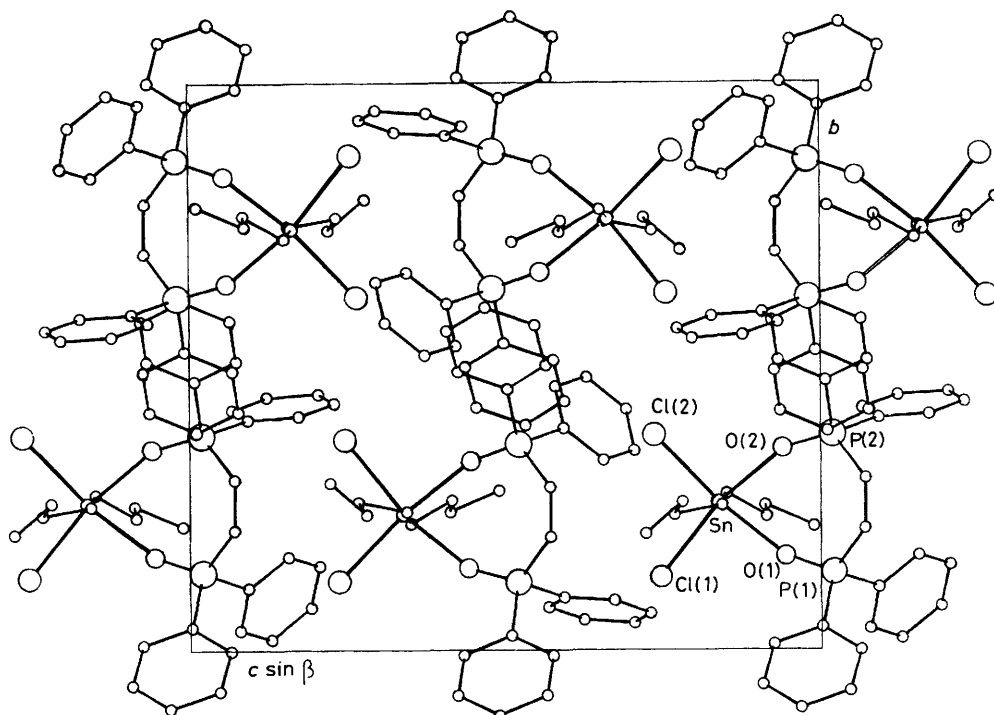


Figure 3. A diagrammatic projection of the structure of $\text{SnBu}^n_2\text{Cl}_2(\text{dpppoet})$ viewed along [100]

O–P–C angles [av. $112.9(6)$ in (1), $113.5(6)^\circ$ in (2)] are the largest and the C–P–C angles [av. $105.8(6)$ in (1), $105.1(6)^\circ$ in (2)] are the smallest; (ii) the disparity in the Sn–O bonds in the two structures has no effect on the P–O bond, 1.48 and 1.50 Å being the values in both compounds; (iii) the P–C bond lengths range from 1.77(1) to 1.81(1) Å in (1), and from 1.77(1) to 1.82(1) Å in (2); (iv) the distances of the P atoms from the phenyl planes do not exceed 0.20 Å; (v) the phenyl rings attached to each P are nearly perpendicular to each other, with angles between the normals to these planes of 92 and 113° in (1), and 95 and 108° in (2); (vi) the P–C–C–P chain is planar in both (1) and (2); and (vii) the Sn–O–P moieties are significantly bent, departing by *ca.* 30° from linearity.

All the carbon atoms of the butyl and propyl chains show large thermal vibration, suggesting some positional disorder.

The crystal structures viewed along [100] for (1) and [001] for (2) are illustrated in Figures 3 and 4, respectively. Molecules are packed with normal van der Waals interactions, the most significant contacts being $\text{Cl}(1) \cdots \text{C}(34)$ ($x, \frac{1}{2} - y, \frac{1}{2} + z$) 3.61(2) Å, $\text{C}(16) \cdots \text{C}(16)$ ($\bar{x}, \bar{y}, \bar{z}$) 3.51(2) Å, and $\text{C}(28) \cdots \text{C}(28)$ ($\bar{x}, 1 - y, \bar{z}$) 3.48(2) Å for (1); $\text{Cl}(2) \cdots \text{C}(32)$ ($x, y, z - 1$) 3.55(1) Å and $\text{Cl}(1) \cdots \text{C}(15)$ ($\bar{x}, \frac{1}{2} + y, \bar{z}$) 3.56(2) Å for (2).

Tin-119 Mössbauer Data.—In light of the known structures, the tin-119 Mössbauer data for the two compounds may be discussed. As can be seen from the data in Tables 7 and 8, both the isomer shift (δ) and quadrupole splitting (Δ) vary little, indicating negligible structural changes over the temperature range studied. The resonance linewidths for (1) are quite narrow (0.93–1.17 mm s^{-1}), but those for (2) steadily increased from the root-mean-squared (r.m.s.) value at 77 K to *ca.* 1.70 mm s^{-1} at 150 K. The quadrupole splitting values of *ca.* 4 mm s^{-1} are of the order expected for a *trans*- SnR_2X_4 arrangement of ligands about tin.²¹ Both complexes, however, show a rapid decrease in resonance area as the temperature increases. We have previously²² demonstrated

Table 7. Tin-119 Mössbauer data for $\text{SnPr}^n_2\text{Cl}_2(\text{dpppoet})$

T/K	δ ^a / mm s^{-1}	Δ ^a / mm s^{-1}	Total resonance area ^b	Relative percentage effect
77.3			27.57 ^c	1.0000
80	1.55	4.00	25.89	0.9391
85	1.56	4.00	24.91	0.9035
90	1.55	3.91	22.19	0.8048
100	1.64	3.82	18.13	0.6576
110	1.55	3.84	15.24	0.5530
120	1.54	3.86	12.87	0.4669
130	1.53	3.86	11.09	0.4024
140	1.60	3.84	9.10	0.3300
150	1.53	3.93	7.69	0.2790

^a ± 0.03 mm s^{-1} . ^b Ratio of higher velocity/lower velocity resonance lines gradually decreases from 0.975 at 80 K to 0.886 at 150 K. ^c Extrapolated value.

that in the temperature range 77–150 K the slopes, a , of the linear portions of the semi-logarithmic plots of relative resonance area, $\ln [A(T)/A(77)]$ versus temperature T , where $A(T)$ is the area of the resonance absorption, are a useful guide to the lattice structure of the material. The values of a are -1.76×10^{-2} and $-1.56 \times 10^{-2} \text{ K}^{-1}$ for the *n*-propyl- and *n*-butyl-tin derivatives, respectively. The latter value is somewhat higher than the value (*ca.* $-1.8 \times 10^{-2} \text{ K}^{-1}$) previously suggested by us from a fairly comprehensive study of compounds of known structure as characteristic of a solid comprising non-interacting molecules. However, several other compounds, also known to be monomeric in the solid state exhibit values higher than this, including tetraphenyltin ($a = -1.659 \times 10^{-2} \text{ K}^{-1}$),²³ the triphenyltin dithiophosphate esters, $\text{SnPh}_3[\text{SP}(=\text{S})(\text{OR})_2]$ ($\text{R} = \text{Et}$, $a = -1.43 \times 10^{-2} \text{ K}^{-1}$; $\text{R} = \text{Pr}^1$, $a = -1.40 \times 10^{-2} \text{ K}^{-1}$),²⁴ and triphenyltin *o*-(2-hydroxy-5-methylphenyl)diazobenzoate ($a = -1.55 \times 10^{-2} \text{ K}^{-1}$).²⁵ The

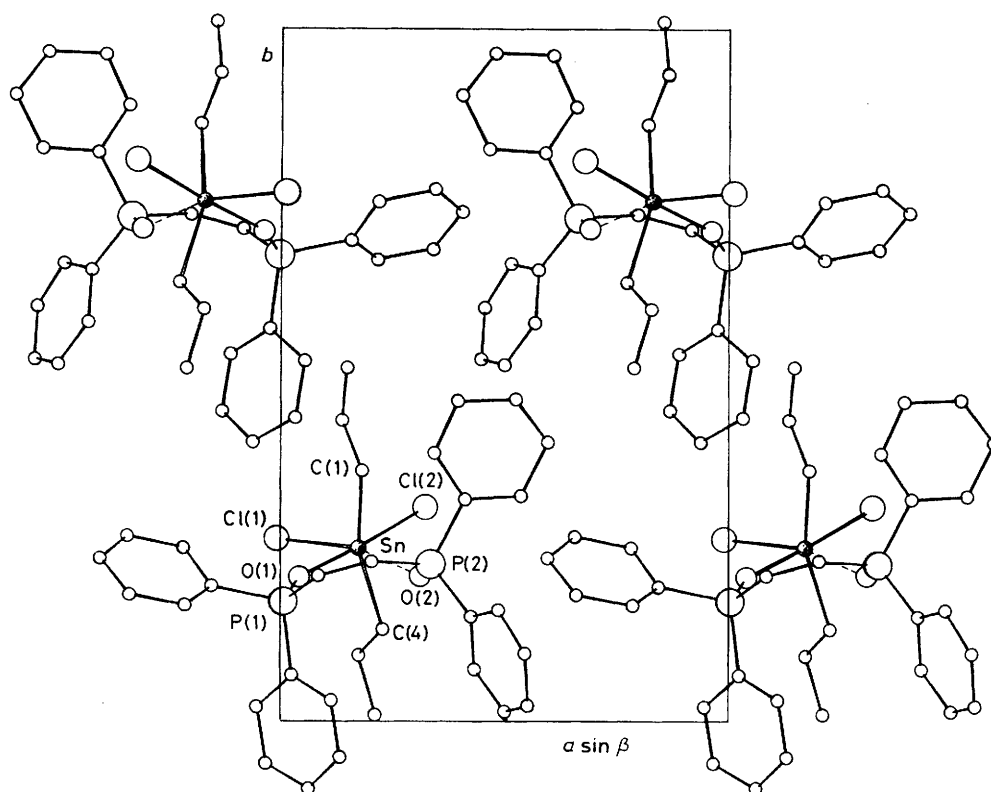


Figure 4. A diagrammatic projection of the structure of $\text{SnPr}^n_2\text{Cl}_2(\text{dppoet})$ viewed along $[001]$

Table 8. Tin-119 Mössbauer data for $\text{SnBu}^n_2\text{Cl}_2(\text{dppoet})$

T/K	$\delta^a/\text{mm s}^{-1}$	$\Delta^a/\text{mm s}^{-1}$	Total resonance area b	Relative percentage effect
77.3			30.30 c	1.0000
80	1.56	4.11	29.27	0.9660
85	1.54	4.11	26.46	0.8733
90	1.53	4.07	24.84	0.8215
100	1.52	4.05	22.12	0.7300
110	1.53	4.08	18.21	0.6010
120	1.53	4.08	16.05	0.5297
130	1.52	4.07	14.13	0.4663
140	1.52	4.09	11.48	0.3789
150	1.52	4.08	9.35	0.3086

$a \pm 0.03 \text{ mm s}^{-1}$; half-height widths fall within the range $0.93\text{--}1.17 \text{ mm s}^{-1}$. b Ratio of higher velocity/lower velocity resonance lines fall within the range $1.12\text{--}1.21$. c Extrapolated value.

higher value of a in these cases was attributed to the efficient packing of the molecules in the crystal lattice, thus restricting their motion. In contrast, molecules of $\text{SnPh}_3(\text{ONPhCOPh})$ and $\text{SnMe}_2(\text{ONMeCOMe})_2$ are much more loosely packed in their respective lattices, and exhibit lower a values of $-1.85 \times 10^{-2} \text{ K}^{-1}$.²² The difference in a values observed for (1) and (2) is unexpectedly large in view of their close constitutional similarity, and, as both complexes possess molecular lattices, this difference must be attributed to the changes in co-ordination around the tin atom. The major difference between the two complexes in this respect is the long Sn-O bond (2.58 \AA) of the propyltin complex, which would permit a greater amplitude of vibration of the tin atom in this direction as the temperature increases, leading to the lower value of a .

That the tin-ligand bond distances within the first co-ordination shell will have a determining effect upon the vibrational amplitude of the tin atom is rather obvious, and is elegantly illustrated by the data for the mixed-valence tin carboxylate, $\text{Sn}^{\text{II}}_2\text{Sn}^{\text{IV}}_2(\mu\text{-O}_2\text{CC}_6\text{H}_4\text{NO}_2\text{-}o)_2(\mu_3\text{-O})_2(\text{thf})_2$ (thf = tetrahydrofuran),²⁶ in which the tin(II) and tin(IV) atoms are in different co-ordination environments within the same molecule. The tin(IV) atoms have almost perfect octahedral co-ordination with Sn-O distances in the range $2.047(6)\text{--}2.067(7) \text{ \AA}$ and exhibit a values of $-1.25 \times 10^{-2} \text{ K}^{-1}$, whilst the tin(II) atoms have pseudo-pentagonal bipyramidal co-ordination with $\text{Sn-O}_{\text{ax}} = 2.113(7) \text{ \AA}$ and $\text{Sn-O}_{\text{eq}} = 2.43(1)\text{--}2.66(1) \text{ \AA}$, with the lone pair occupying the second axial site, and exhibit a higher a value of $-1.65 \times 10^{-2} \text{ K}^{-1}$.

Finally, the root-mean-square amplitude of vibrations of the tin atom, $\langle x(T) \rangle$, and the absolute value of the recoil-free fraction of the tin nuclide, $f(T)$, may be estimated using the relationship, $f(T) = \exp[-\langle x(T)^2 \rangle / \lambda^2]$, where λ is the wavelength of the Mössbauer transition divided by 2π , using the room-temperature crystallographic vibrational amplitude as a datum point. For $\text{SnPr}^n_2\text{Cl}_2(\text{dppoet})$, the r.m.s. value at 290 K (0.200 \AA) corresponds to a value of f of 0.0028 , reducing to 0.177 \AA at 77 K , when $f = 0.0101$. This value may be compared to that derived for the $\text{SnBu}^n_2\text{Cl}_2(\text{dppoet})$ complex at 77 K ($f = 0.0438$), which possesses a one-dimensional polymeric structure, with a bridging rather than a chelating ligand, leading to more restricted motion and a higher f value.¹ Similar estimations were not possible for $\text{SnBu}^n_2\text{Cl}_2(\text{dppoet})$ because of the lower quality of the crystallographic data.

Acknowledgements

This investigation was supported by an International Grant of the National Research Council (Rome).

References

- 1 Part 1, P. G. Harrison, N. W. Sharpe, C. Pelizzi, G. Pelizzi, and P. Tarasconi, *J. Chem. Soc., Dalton Trans.*, 1983, 921.
- 2 M. Mathew and G. J. Palenik, *Inorg. Chim. Acta*, 1971, **5**, 573.
- 3 A. E. Kalinin, V. G. Andrianov, and Yu. T. Struchkov, *Zh. Strukt. Khim.*, 1976, **17**, 153.
- 4 J. S. Field, P. J. Wheatley, and S. Bhaduri, *J. Chem. Soc., Dalton Trans.*, 1974, 74.
- 5 S. Z. Goldberg and K. N. Raymond, *Inorg. Chem.*, 1973, **12**, 2923.
- 6 M. Nardelli, C. Pelizzi, and G. Pelizzi, *Inorg. Chim. Acta*, 1979, **33**, 181.
- 7 C. Pelizzi and G. Pelizzi, *J. Organomet. Chem.*, 1980, **202**, 411.
- 8 C. Pelizzi and G. Pelizzi, *Inorg. Nucl. Chem. Lett.*, 1980, **16**, 451.
- 9 W. E. Slinkard and D. W. Meek, *J. Chem. Soc., Dalton Trans.*, 1973, 1024.
- 10 M. S. Lehmann and F. K. Larsen, *Acta Crystallogr., Sect. A*, 1974, **30**, 580.
- 11 D. Belletti, F. Uguzzoli, A. Cantoni, and G. Pasquinelli, Gestione on Line di Difrattometro a Cristallo Singolo Siemens AED con Sistema General Automation Jumbo 220, Internal Reports, 1979.
- 12 G. M. Sheldrick, SHELX 76, Program for Crystal Structure Determination, University of Cambridge, 1976.
- 13 S. S. Sandhu and S. S. Sandhu, *J. Inorg. Nucl. Chem.*, 1969, **31**, 1363.
- 14 E. I. Sinyavskaya and Z. A. Shcheka, *Russ. J. Inorg. Chem.*, 1976, **21**, 1330.
- 15 A. J. Crowe, P. J. Smith, and P. G. Harrison, *J. Organomet. Chem.*, 1981, **204**, 327.
- 16 R. C. Poller and J. N. R. Ruddick, *J. Chem. Soc. A*, 1969, 2273.
- 17 K. L. Jaura, K. Chander, and K. K. Sharma, *Z. Anorg. Allg. Chem.*, 1970, **376**, 303.
- 18 T. Tanaka, *Inorg. Chim. Acta*, 1967, **1**, 217.
- 19 V. G. Kumar Das, *J. Inorg. Nucl. Chem.*, 1976, **38**, 1241.
- 20 C. A. L. Filgueiras, C. Celso, E. V. Marques, and B. F. G. Johnson, *Inorg. Chim. Acta*, 1982, **59**, 71.
- 21 G. M. Bancroft, V. G. Kumar Das, T. K. Sham, and M. G. Clark, *J. Chem. Soc., Dalton Trans.*, 1976, 643.
- 22 P. G. Harrison, R. C. Phillips, and E. W. Thornton, *J. Chem. Soc., Chem. Commun.*, 1977, 603.
- 23 R. H. Herber and M. F. Leahy, *J. Chem. Phys.*, 1977, **67**, 2718.
- 24 J. L. Lefferts, K. C. Molloy, J. J. Zuckerman, I. Haiduc, C. Guta, and D. Ruse, *Inorg. Chem.*, 1980, **19**, 1662.
- 25 P. G. Harrison, K. Lambert, T. J. King, and B. Majee, unpublished work.
- 26 P. F. R. Ewnigs, P. G. Harrison, A. Morris, and T. J. King, *J. Chem. Soc., Dalton Trans.*, 1976, 1602.

Received 27th September 1982; Paper 2/1651